Appl. Phys. B 86, 337–341 (2007)
DOI: 10.1007/s00340-006-2526-1

Applied Physics B
Lasers and Optics

R.A. GANEEV[1,✉]
A.I. RYASNYANSKIY[2,3]
U. CHAKRAVARTY[4]
P.A. NAIK[4]
H. SRIVASTAVA[4]
M.K. TIWARI[4]
P.D. GUPTA[4]

Structural, optical, and nonlinear optical properties of indium nanoparticles prepared by laser ablation

[1] Akadempribor Scientific Association, Academy of Sciences of Uzbekistan, Akademgorodok, Tashkent 700125, Uzbekistan
[2] Samarkand State University, 703004 Samarkand, Uzbekistan
[3] Institut des Nano-Sciences de Paris, CNRS-Université Pierre et Marie Curie, 75015 Paris, France
[4] Raja Ramanna Centre for Advanced Technology, Indore 452013, India

Received: 26 May 2006/Revised version: 25 October 2006
Published online: 13 December 2006 •

ABSTRACT A study of indium nanoparticles prepared by two laser ablation techniques is reported. The suspensions of indium nanoparticles were prepared using the laser ablation of bulk indium in liquids. The prepared suspensions of indium nanoparticles were analyzed by the X-ray fluorescence spectroscopy and absorption spectroscopy. The position of the surface plasmon resonance of In-containing suspensions (350 nm) was consistent with the estimations taking into account the average size of In nanoparticles (43 nm) measured using the X-ray fluorescence spectroscopy. The nonlinear optical parameters of indium nanoparticles-containing liquids were studied by the *z*-scan technique using a picosecond Nd:YAG laser. We compare the laser ablation in liquids with the laser ablation of indium in vacuum at the tight and weak focusing conditions of a Ti:sapphire laser and analyze the 60 nm indium nanoparticles synthesized in the latter case.

PACS 42.65.An; 42.65.Hw; 42.65.Jx; 61.46.Df; 78.67.Bf

1 Introduction

The nanostructures of different materials are of special interest in nonlinear optics and optoelectronics. The quantum confinement effect is responsible for the variation and enhancement of their structural, optical, and nonlinear optical characteristics compared to those of the bulk materials. Silver [1, 2], copper [2–4], and gold [2, 5] are among the most useful metals suited for the nanoparticles preparation for the optoelectronics and nonlinear optics. The nanoparticle-containing composites based on other metals (Co [6], Sn [7], Fe [8], Ni [4]) have also been studied and these have also exhibited high values of nonlinear optical susceptibilities. Further search of prospective nanoparticle-containing materials and their preparation and application are of considerable importance nowadays. For example, metal nanoparticles will be potential additives of lubricating oils in the near future; indium nanoparticles are expected to play a part in future nanometer lubricants. The indium nanoparticles could also be used for single electron transistors, as tags for detection of DNA hybridization, as printing building blocks in nanoxerography, and as starting material for convenient synthesis of InP using phosphide ions.

The past studies on the preparation of indium nanoparticles using the metal vapor deposition [9], reduction of $InCl_3$ by alkalides [10], and solution dispersion method [11] have revealed the interesting structural and optical properties of these samples. The laser ablation of metals in liquids is among the new techniques, which can also be applied for the preparation of indium nanoparticles-containing media. Recently, the application of this method for the preparation of semiconductor [12–14] and metal [15] colloids has been demonstrated.

The "cost" of laser ablation in liquids as a simpler preparation method in the terms of the properties of nanoparticles is relatively stable in the short-term. This is a main obstacle of laser ablation in liquids. It would be problematic for technological applications of the material in the case when optical properties of nonlinear device containing such structures appear to be unstable under long-term laser irradiation. One of possible proposals to overcome this obstacle is a preparation of the nanoparticles containing In solution using low viscosity liquid and further dissolution of prepared solution in the matrix with high viscosity.

To examine the generality of the method and its potential use for preparing nanoparticles, we considered indium, which has a low melting point metal, is a good candidate for such studies and can be of various practical interests. Indium nanoparticles have been prepared by some other methods also [9–11, 16–18]. In [11], small indium particles were prepared by metal vapor deposition. Indium nanoparticles were also prepared by the evaporation of indium into a polymerized monomer in order to study the thermal stability of the resulting composite material [16]. The description of the synthesis of monodispersed indium nanoparticles by an organometallic route and their arrangement in two- and three-dimensional networks is presented in [17]. The method for indium nanoparticles preparation from bulk indium that involves surface oxidation and dispersion of indium droplets is described in [11].

✉ Fax: +998-71-1690124, E-mail: rashid_ganeev@yahoo.com

In the present work, the indium nanoparticles were prepared by laser ablation in liquids. The structural, optical and nonlinear optical properties of the solutions of these nanoparticles are reported. The structural properties of the deposited indium nanoparticles-containing films prepared by the laser ablation of bulk indium target in the vacuum at the tight and weak focusing conditions are also analyzed.

2 Experimental configuration

A nanosecond Nd:YLF laser (pulse duration $t = 20$ ns, wavelength $\lambda = 1054$ nm, pulse energy $E = 36$ mJ, 10 Hz pulse repetition rate) was used for the ablation of indium target in liquids. The laser radiation was focused by a 6 cm focal length lens inside a 5 cm long cell containing ethanol or water. The bulk indium to be ablated was kept close to the back window of the cell, to prevent any optical damage of the input window. The ablation was performed at an energy density of 20 Jcm^{-2} for 15 min (9000 laser shots), after which a yellow-colored suspension was obtained. It may be noted that an increase in the ablation time resulted in a decrease in the efficiency of the nanoparticles formation and also led to sedimentation of large nano-aggregates. The absorption spectrum of the prepared nanoparticle-containing suspensions was recorded using a fiber optical spectrograph (USB2000: Ocean Optics). The structural analysis of In nanoparticles sizes was carried out using the total reflection X-ray fluorescence spectrometry (TXRF). Details of the TXRF are described in [19].

The investigation of the nonlinear optical characteristics of indium nanoparticles suspensions was carried out using the second harmonic of the picosecond Nd:YAG laser radiation (532 nm) and standard z-scan technique [20]. The description of the experimental procedure for the measurements of the nonlinearities of such structures can be found elsewhere [21]. Note that due care was taken to prevent any optical breakdown in the indium-containing suspensions. The breakdown intensity of such structures was measured to be $(2\text{–}3)\times10^{10}$ Wcm^{-2}, while the laser intensities used in our nonlinear optical studies did not exceed $(2\text{–}4)\times10^{9}$ Wcm^{-2}.

To compare the properties of the indium nanoparticle suspension in liquids with the vacuum evaporated indium nanoparticles, deposition of indium on different substrates was carried out in a vacuum chamber. In this case, Ti:sapphire laser chirped pulses ($\lambda = 793$ nm, $t = 200$ ps, $E = 30$ mJ, 10 Hz pulse repetition rate) were focused on the bulk indium target at two regimes of focusing. In the first case (tight focusing), the intensity of laser radiation was 3×10^{12} Wcm^{-2}, and in the second case (weak focusing), the intensity was considerably lower (4×10^{10} Wcm^{-2}). Float glass, silicon wafer, and various metal strips (silver, copper, aluminum) were used as the substrates, and were placed at a distance of 50 mm from the ablated indium target.

The structures of ablated indium were analyzed by studying the deposited films on different substrates. The nature of the nanoparticles is determined by the thermodynamic conditions at the target surface. The presence of nanoparticles was checked by analyzing the spatial characteristics of deposited material. The structural properties of deposited films were analyzed by scanning electron microscopy (SEM, Philips XL30CP), transmission electron microscopy (TEM, Philips CM200), and TXRF.

3 Results and discussion

Much attention has been devoted during the past few years to precise spatial arrangement in two- and three-dimensional superlattice structures of metals. However, ordering and exploitation of the nanomaterials necessitates the synthesis of monodispersed individual particles, for which no general method is presently available. We describe later in the text the analysis of synthesized indium nanoparticles by laser ablation of bulk indium at two different conditions of ablation.

The absorption spectrum of the ethanol suspension of ablated indium is presented in Fig. 1. The observed absorption maximum at 350 nm can be associated with the surface plasmon resonance (SPR) of indium nanoparticles. A broad SPR peak indicates the presence of the nanoparticles with different sizes.

The absorption spectra of indium nanoparticles dispersed in chloroform exhibiting the characteristic peak of the surface plasmon band at 240 nm, which reveals the formation of indium particles, were reported in [11]. They have mentioned that the surface plasmon band at 240 nm is a clear evidence for the existence of the individual particles less than 50 nm in size. In addition, UV absorption measurements at room temperature presented in [18] have shown surface plasmon bands characteristic for the specific nanoparticle size. Surface plasmon bands were observed by them at 281 nm (for the 1.3 nm average particle size), 291 nm (for the 12 nm average particle size) and 319, 340 and 350 nm (for the 107 nm average particle size) respectively.

The surface plasmon properties of quantum confined structures have been explained by Kreibig and Genzel [22]. As the mean free path of the metal electrons exceeds the particle size, the free-electron contribution to the dielectric function undergoes a modification, thereby causing the surface plasmon resonance frequency peak to be directly proportional to the particle size and the resonance spectral width to be inversely proportional to the particle size [22, 23].

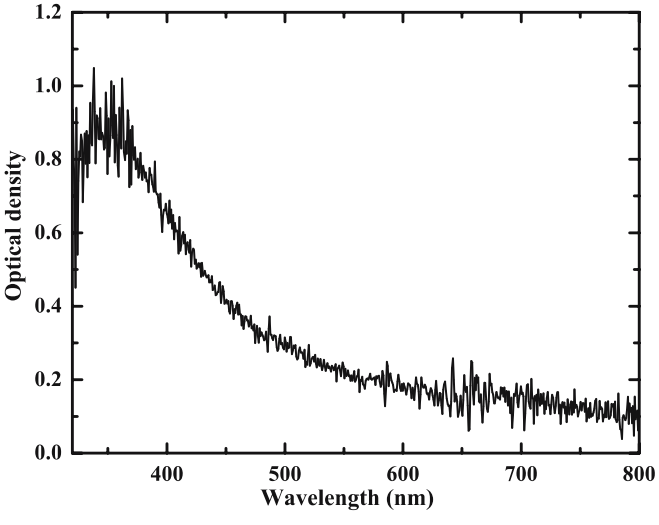

FIGURE 1 Absorption spectrum of ablated indium suspension in ethanol

For the sizes of measured In nanoparticles (43 nm) the quantum effects do not take place. The role of higher sized nanoparticles could lead to the red-shift of the absorption peak. At the same time, previous studies of the surface plasmon resonance of indium nanoparticles have shown that it shifts toward the longer wavelength range both in the case of different solvents [24] and morphologies [25] of In clusters, and for different techniques for the preparation of nanoparticles. When the In clusters are embedded in the matrix with a high refractive index, the Mie resonances can also be down-shifted to the visible range. At the same time, the absorption phenomenon in indium nanoparticles due to surface plasmon resonance is found solvent dependent [24]. Shift of about 50 nm for this absorption for In in dichloromethane (290 nm) probably indicates the formation of larger sized indium particles thus corroborating with the early reports (240 nm [11, 26]).

The indirect confirmation of the variation of the SPR is also presented in the case of reflectance anisotropy spectroscopy of the In islands on GaAs surface, wherein, for higher indium coverage, the shift of the reflectance anisotropy spectra from 250 nm to 400 nm was observed [27].

Probably, in our case, the reason of the shift of the resonance from 240 nm to 350 nm range was caused by different morphology of the particles (e.g., varied from spherical to elliptical shape), as it was discussed in literature in the case of silver nanoparticles.

Total reflection X-ray fluorescence measurements were performed using an in-house developed TXRF spectrometer [28]. Angle dependence of the fluorescence intensity in the total reflection region can behave in several ways [29, 30]. It can also be successfully used to identify presence of nanoparticles on a flat surface. The structure of indium nanoparticles prepared by laser ablation process was analyzed using TXRF spectrometry.

The fluorescence measurements were carried out using a Peltier cooled solid state detector (EurisusMesures EPXR 10-300), a spectroscopy amplifier AMP 6300 and a multichannel pulse height analyzer installed in a personal computer. The solid state detector had an energy resolution of 250 eV at 5.9 keV. A well-collimated primary beam, from a line focus Cu X-ray tube, was used as an excitation source. Figure 2 shows the X-ray fluorescence trace recorded in the case of indium nanoparticles deposited after evaporation from the liquid suspension on a plexiglass substrate. It can be seen from Fig. 2 that, below the critical angle of the plexiglass substrate ($\sim 0.17^\circ$) the angle dependent fluorescence profile of indium shows oscillations. These oscillations are mainly due to the presence of nanostructure on the flat surface. The average size of the indium nanoparticles was determined by fitting the recorded fluorescence profile using CATGIXRF program [31]. Solid line presents the best theoretical fit, from which the average size of the nanoparticles was estimated to be 43 nm. The TEM measurements also confirmed the presence of indium nanoparticles in the prepared suspensions, with effective size distribution lying between 20 nm to 100 nm.

The results of the measurements of the nonlinear optical parameters of indium nanoparticles-containing aqueous suspension are presented in Fig. 3. The closed-aperture

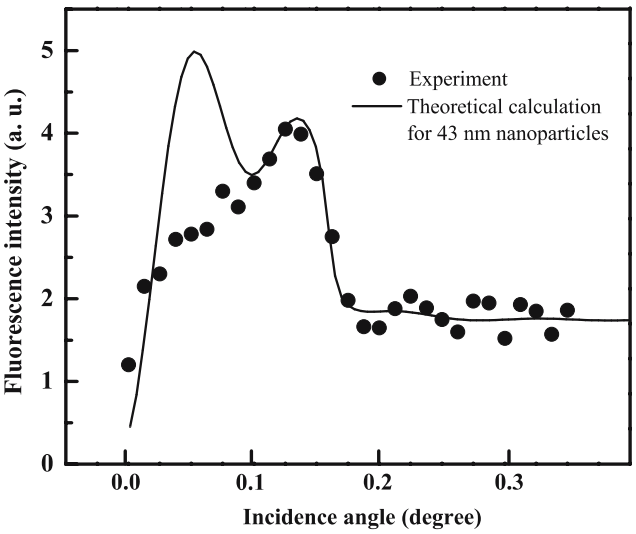

FIGURE 2 Recorded fluorescence profile of the indium nanoparticles prepared by laser ablation in alcohol and deposited on the plexiglass substrate. The *scattered points* show experimental data, while the *solid line* shows a fitted profile. The critical angle of plexiglass is $\sim 0.17^\circ$ for 8.50 keV X-ray energy

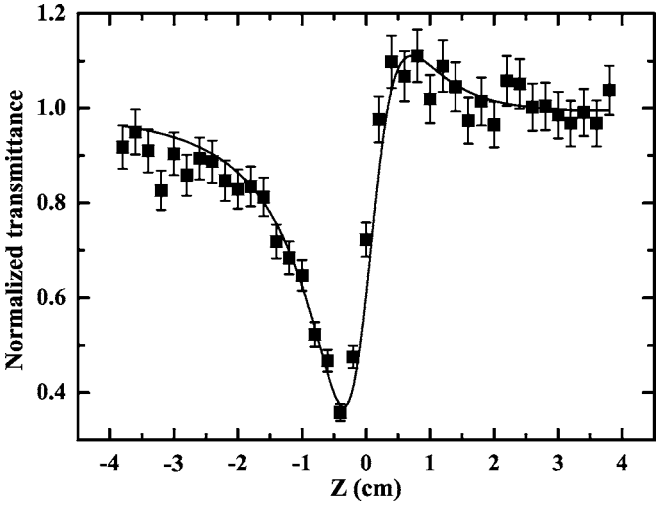

FIGURE 3 Closed-aperture z-scan of indium nanoparticle-containing aqueous suspension. *Solid line* is the best theoretical fit

z-scan shows a minimum of a normalized transmittance $T(z)$ before the focal position with further maximum after the focus, which characterizes a medium having a positive nonlinear refractive index. At the same time, the minimum peak considerably exceeded the maximum peak, which indicates nonlinear absorption in the prepared suspension. The influence of thermal nonlinearity was insignificant, since we used the Nd:YAG laser (50 ps) in a low-repetition rate of 2 Hz.

By defining the relative coordinate $x = z/z_0$, z_0 being the diffraction length, the dependence of the normalized closed-aperture transmission T in the case of nonlinear refraction can be written as [32]

$$T(x) = 1 - \frac{4x}{(x^2+9)(x^2+1)}\Delta\Phi_0 - \frac{2(x^2+3)}{(x^2+9)(x^2+1)}\Delta\Psi_0 \tag{1}$$

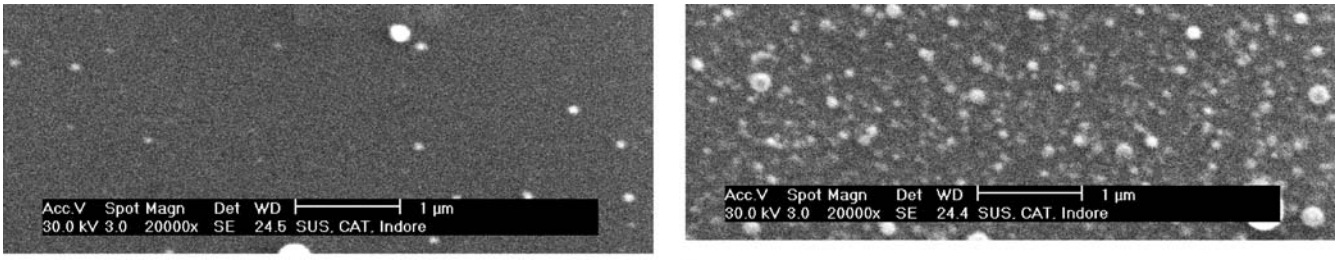

a **b**

FIGURE 4 SEM images of the deposited indium nanoparticles on the surface of Si wafer. These images were obtained at (**a**) weak and (**b**) tight focusing conditions

Here $z_0 = 0.5kw_0^2$, $\Delta\Phi_0 = k\gamma I_0 L_{\text{eff}}$, $\Delta\psi_0 = \beta I_0 L_{\text{eff}}/2$, γ and β are the nonlinear refractive index and nonlinear absorption coefficient of the medium, respectively, $k = 2\pi/\lambda$ is the wave number, w_0 is the beam waist radius at the beam focus, $L_{\text{eff}} = [1 - \exp(-\alpha_0 L)]/\alpha_0$ is the effective sample length, L is the medium length (in our case L is the thickness of the cell with indium nanoparticles, $L = 2$ mm) and α_0 is the linear absorption coefficient, which was calculated from the absorption spectra of the samples.

The best theoretical fit of the (1) with the experimental measurements (Fig. 3, solid line) gave the nonlinear optical parameters of the solution $\{\gamma = (1.24 \pm 0.41) \times 10^{-18}\,\text{m}^2\text{W}^{-1}$ and $\beta = (1.02 \pm 0.2) \times 10^{-11}\,\text{mW}^{-1}\}$. The values of the real and imaginary parts of the third-order nonlinear susceptibilities were calculated to be $9.9 \times 10^{-22}\,\text{m}^2\text{V}^{-2}$ and $3.43 \times 10^{-22}\,\text{m}^2\text{V}^{-2}$, respectively. Using these data points, the absolute value of $\chi^{(3)}$ was calculated to be $1.05 \times 10^{-21}\,\text{m}^2\text{V}^{-2}$. One can see that the value of $|\chi^{(3)}|$ is mostly dependent on the nonlinear refractive properties of indium nanoparticles-containing solution. The relatively small value of optical nonlinearities was defined by the small volume part of the indium nanoparticles in the solution ($\sim 10^{-5}$). Taking into account this value, one can estimate the nonlinear susceptibility of indium nanoparticles to be $1.05 \times 10^{-16}\,\text{m}^2\text{V}^{-2}$.

Our studies of the structural properties of the deposited indium film showed that, in the case of tight focusing conditions, these films contain a lot of nanoparticles with variable sizes. In the case of weak focusing conditions, the concentration of nanoparticles was considerably smaller compared to the tight focusing conditions. Figure 4 shows the SEM images of the deposited indium nanoparticles on the surface of Si wafer. In the case of weak focusing, the deposited film was almost homogeneous with a few nanoparticles appearing in the SEM images, while, at tight focusing conditions, a plenty of the nanoparticles ranging from 30 to 100 nm appeared in the SEM images. The average size of these nanostructures was estimated to be 60 nm. Analogous results were observed using the TEM and TXRF. In particular, the TXRF was taken for deposition on a glass slide at the weak focusing condition and on a float glass at the tight focusing condition. Figure 5 shows In $L\alpha$ fluorescence intensity as a function of the incidence angle in the TXRF set-up for the weak focusing condition. It can be seen from this figure that the fluorescence intensity decreased abruptly below the critical angle ($\sim 0.36°$) for indium. For incidence angles larger than the critical angle, In $L\alpha$ fluorescence intensity increased monotonically. This behavior is like that of a thick film of indium deposited on the substrate. If the indium were present in the form of nanoparticles, it would have shown a profile similar to that in Fig. 2. In fact, for the tight focusing condition, we could infer formation of nanoparticles in the deposition made on float glass from the observed variation of In $L\alpha$ fluorescence intensity with respect to the incidence angle.

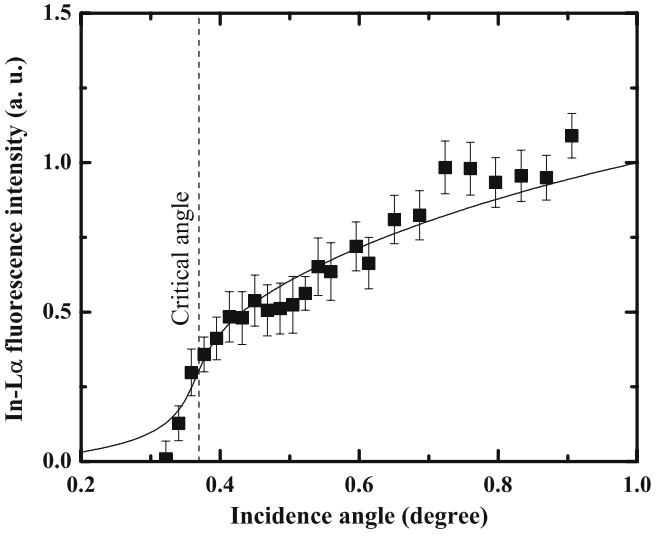

FIGURE 5 Recorded X-ray fluorescence profile from a sample prepared at the weak focusing conditions. This figure shows that the indium is deposited in the form of a thick monoatomic film instead of nanoparticles. The experimental data are plotted with the respective uncertainties whereas the solid line shows a fitted profile. The critical angle of indium is $\sim 0.36°$ for 8.50 keV X-ray energy

Our studies show that, even by using long laser pulses, the nanoparticles formation is realized at strong laser focusing, which was previously reported mostly using ultrashort laser pulses. The most interesting and new features of laser ablation and nanoparticles formation during irradiation of the solid targets have been recently observed in the case of 100 fs–1 ps laser pulses. In the present work, we analyze the conditions when In nanoparticles were prepared by the sub-nanosecond laser ablation of the target placed in vacuum. The effect of focusing condition of the laser (tight or weak focusing) on the films and nanoparticles prepared by the laser ablation of bulk targets in the vacuum is analyzed. Our results show that, as well as in previously reported studies using ultrashort laser pulses, the long laser pulses at tight focusing conditions could also be used for the nanoparticles formation.

4 Conclusions

In conclusion, a study of indium nanoparticles prepared by laser ablation of bulk indium at different conditions is presented. In the case of laser ablation of bulk indium in liquids, nanoparticles suspensions were analyzed for nonlinear optical coefficients using the z-scan technique. The z-scan profile indicated positive nonlinear refraction and gave estimates of the nonlinear absorption characteristics of indium suspension $\{\gamma = (1.24 \pm 0.41) \times 10^{-18}\,\mathrm{m^2W^{-1}}$, $\beta = (1.02 \pm 0.2) \times 10^{-11}\,\mathrm{mW^{-1}}\}$. The nonlinear susceptibility of indium nanoparticles was estimated to be $1.05 \times 10^{-16}\,\mathrm{m^2V^{-2}}$, taking into account a small volume part of nanoparticles in the solution ($\sim 10^{-5}$). The average size of indium nanoparticles in suspension, measured using XRF spectrometry (43 nm), was comparable with that inferred from the analysis of the absorption spectra of indium suspension. The indium nanoparticles displayed a strong SPR absorption band at 350 nm.

The study of the indium nanoparticles prepared at the conditions of laser ablation in vacuum using picosecond pulses showed a considerable difference in the structural properties of the deposited films. In the case of weak focusing conditions, when only excited In atoms and a small amount of In II ions was observed from the plasma spectrum, the concentration of nanoparticles was considerably smaller compared to the tight focusing conditions. The average size of nanoparticles in the latter case was measured to be 60 nm.

ACKNOWLEDGEMENTS R.A. Ganeev gratefully acknowledges the invitation and support from Raja Ramanna Centre for Advanced Technology, Indore, India to carry out this work. Thanks are also due to R.V. Nandedkar of RRCAT for his help in taking SEM images and TXRF data. A.I. Ryasnyanskiy thanks INTAS foundation for financial support (Grant N 05-109-4749).

REFERENCES

1 R.A. Ganeev, A.I. Ryasnyanskiy, A.L. Stepanov, T. Usmanov, Opt. Quantum Electron. **36**, 949 (2004)
2 R.A. Ganeev, A.I. Ryasnyansky, A.L. Stepanov, C. Marques, R.C. da Silva, E. Alves, Opt. Commun. **253**, 205 (2005)
3 I. Ryasnyansky, B. Palpant, S. Debrus, R.A. Ganeev, A.L. Stepanov, N. Can, C. Buchal, S. Uysal, Appl. Opt. **44**, 2839 (2005)
4 M. Falconieri, G. Salvetti, E. Cattaruza, F. Gonella, G. Mattei, P. Mazzoldi, M. Piovesan, G. Battaglin, R. Polloni, Appl. Phys. Lett. **73**, 288 (1998)
5 S. Debrus, J. Lafait, M. May, N. Pinçon, D. Prot, C. Sella, J. Venturini, J. Appl. Phys. **88**, 4469 (2000)
6 E. Cattaruzza, F. Gonella, G. Mattei, F. Mazzoldi, D. Gatteschi, C. Sangregorio, M. Falconieri, G. Salvetti, G. Battaglin, Appl. Phys. Lett. **73**, 1176 (1998)
7 D. Ila, E.K. Williams, S. Sarkisov, C.C. Smith, D.B. Poker, D.K. Hensley, Nucl. Instrum. Methods Phys. Res. B **141**, 289 (1998)
8 W. Wang, G. Yang, Z. Chen, Y. Zhou, H. Lu, G. Yang, J. Appl. Phys. **92**, 7242 (2002)
9 Q. Chen, M. Tanaka, K. Furuya, J. Surf. Anal. **5**, 348 (1999)
10 K.-L. Tsai, J.L. Dye, J. Am. Chem. Soc. **113**, 1650 (1991)
11 Y. Zhao, Z. Zhang, H. Dang, J. Phys. Chem. B **107**, 7574 (2003)
12 R.A. Ganeev, A.I. Ryasnyanskiy, R.I. Tugushev, T. Usmanov, J. Opt. A **5**, 409 (2003)
13 R.A. Ganeev, M. Baba, A.I. Ryasnyansky, M. Suzuki, H. Kuroda, Appl. Phys. B **80**, 595 (2005)
14 R.A. Ganeev, A.I. Ryasnyansky, Opt. Commun. **246**, 163 (2005)
15 R.A. Ganeev, M. Baba, A.I. Ryasnyansky, M. Suzuki, H. Kuroda, Opt. Commun. **240**, 437 (2004)
16 G.T. Cardenas, E.C. Salgado, J. Morales, H.Z. Soto, J. Appl. Polym. Sci. **73**, 1239 (1999)
17 K. Soulantica, A. Maisonnat, M.-C. Fromen, M.-J. Casanove, P. Lecante, B. Chaudret, Angew. Chem. Int. Edit. **40**, 448 (2001)
18 Meliorum Technologies Proprietary, http://www.meliorum.com
19 M.K. Tiwari, K.J.S. Sawhney, B. Gowri Sankar, V.K. Raghuvanshi, R.V. Nandedkar, Spectrochim. Acta B **59**, 1141 (2004)
20 M. Sheik-Bahae, A.A. Said, T.-H. Wei, D.J. Hagan, E.W. Van Stryland, IEEE J. Quantum Electron. **QE-26**, 760 (1990)
21 R.A. Ganeev, A.I. Ryasnyansky, S.R. Kamalov, M.K. Kodirov, T. Usmanov, J. Phys. D Appl. Phys. **34**, 1602 (2001)
22 U. Kreibig, L. Genzel, Surf. Sci. **156**, 678 (1985)
23 C.F. Bohren, D.R. Huffman, *Absorption and Scattering of Light by Small Particles* (Wiley, New York, 1983)
24 P.K. Khanna, K.-W. Jun, K.B. Hong, J.-O. Baeg, R.C. Chikate, B.K. Das, Mater. Lett. **59**, 1032 (2005)
25 T.V. Shubina, D.S. Plotnikov, A. Vasson, J. Leymarie, M. Larsson, P.O. Holtz, B. Monemar, H. Lu, W.J. Schaff, P.S. Kop'ev, J. Cryst. Growth **288**, 230 (2006)
26 T.S. Anderson, R.H. Magruder, R.A. Week, R.A. Zuhr, J. Non-Cryst. Solids **203**, 114 (1996)
27 N. Esser, A.M. Frisch, A. Röseler, S. Schintke, C. Goletti, B.O. Fimland, Phys. Rev. B **67**, 125 306 (2003)
28 M.K. Tiwari, B. Gowrishankar, V.K. Raghuvanshi, R.V. Nandedkar, K.J.S. Sawhney, Bull. Mater. Sci. **25**, 435 (2002)
29 M.J. Bedzyk, G.M. Bommarito, J.S. Schildkraut, Phys. Rev. Lett. **62**, 1376 (1989)
30 D.K.G. de Boer, Phys. Rev. B **44**, 498 (1991)
31 M.K. Tiwari, Calculation of Grazing Incidence X-ray Fluorescence Intensities from a Layer Samples, RRCAT Internal Report, Indore, India (2006)
32 X. Liu, S. Guo, H. Wang, L. Hou, Opt. Commun. **197**, 431 (2001)